Room temperature synthesis of porous SiO_2 thin films by plasma enhanced chemical vapor deposition

A. Barranco
Instituto de Ciencia de Materiales de Sevilla (CSIC-Universidad de Sevilla) Avda, Américo Vespucio s/n, E-41092 Sevilla, Spain and Dpto. de Química Inorgánica, Facultad de Química, Avda, Reina Mercedes s/n, Sevilla, Spain

J. Cotrino
Instituto de Ciencia de Materiales de Sevilla (CSIC-Universidad de Sevilla) Avda, Américo Vespucio s/n, E-41092 Sevilla, Spain and Dpto. de Física Atómica, Molecular y Nuclear, Facultad de Física, Universidad de Sevilla, Avda, Reina Mercedes s/n, Sevilla, Spain

F. Yubero, J. P. Espinós, and A. R. González-Elipe[a)]
Instituto de Ciencia de Materiales de Sevilla (CSIC-Universidad de Sevilla) Avda, Américo Vespucio s/n, E-41092 Sevilla, Spain and Dpto. de Química Inorgánica, Facultad de Química, Avda, Reina Mercedes s/n, Sevilla, Spain

(Received 10 July 2003; accepted 19 April 2004; published 16 July 2004)

Silicon dioxide thin films with variable and controlled porosity have been prepared at room temperature by plasma enhanced chemical vapor deposition in an electron cyclotron resonance microwave reactor with a downstream configuration. The procedure consists of the deposition of successive cycles consisting of a sacrificial organic-polymeric layer and, afterward, a silicon dioxide layer. Toluene and oxygen are used as precursors of the organic layers and $Si(CH_3)_3Cl$ and oxygen for the SiO_2. During deposition of the latter, the organic layer is simultaneously burned off. In these conditions, the release of gases produced by oxidation of the organic-polymeric layer take place while the oxide layer is being deposited. Thus, modification of the nucleation and growing mechanism of the silicon oxide thin film take place. The porosity of the final porous SiO_2 thin films increases with the thickness of the sacrificial organic layer. The porous SiO_2 films prepared with the aforementioned method are free of carbon and chlorine contamination as confirmed by Fourier-transform infrared spectroscopy, x-ray photoelectron spectroscopy, and Rutherford backscattering spectroscopy. Depending on their porosity, the SiO_2 thin films are either transparent or scattered visible light. The former have refractive index lower than that of thermal silicon dioxide and the latter show membranelike behavior in gas diffusion experiments. All the samples have good adhesion to the substrates used for the deposition, either polished Si wafer, glass plates, or standard porous supports. They have columnar microstructure, as determined by scanning electron microscopy. A preliminary ultraviolet-visible characterization of the optically transparent thin films reveals that transmission of light through glass increases by 7%–8% when the porous silica is deposited on this substrate. These films prove to be very efficient as antireflective coatings and are of interest for photovoltaic and similar applications. It is possible to deposit SiO_2 thin films with densities as low as 0.65 g/cm^3 (corresponding to a porosity of 70%) by adjusting the thickness of the sacrificial and SiO_2 layers. The films with high porosity are promising materials for the fabrication and/or modification of diffusion membranes. The gas adsorption properties and the type of porosity of the SiO_2 thin films are assessed by adsorption isotherms of toluene at room temperature measured with a quartz crystal monitor device. The gas permeation properties of the films (when used as membranes) are analyzed by studying the diffusion rate of different gases through them. © *2004 American Vacuum Society.* [DOI: 10.1116/1.1761072]

I. INTRODUCTION

Fabrication of porous metal oxide thin films with controlled porosity has received much attention during recent years. They are used as antireflective coatings in optics and photovoltaic applications,[1–3] and in electronics as low-k materials,[4–6] where relatively thin films are deposited on compact substrates. They are also used as diffusion membranes for separation and purification of fluids.[7–10] In this latter case, thicker films deposited on porous and polycrystalline substrates are required. Furthermore porous layers are used as biosubstrates since the roughness of substrates is a very effective parameter to control the growth and proliferation of cells.[11]

Porous SiO_2 thin films used as membranes or similar applications can be prepared by either wet (sol-gel, etc.) or dry procedures.[3,7–10] Wet routes have been also used for the preparation of many other oxide thin films with controlled microstructure and porosity.[10,12–15] When using sol-gel and other wet or ceramic methods, the synthesis of membrane films involves some heating stages to remove solvents, in-

[a)]Author to whom correspondence should be addressed; electronic mail: agustin@cica.es

duce sintering, etc., particularly if the substrate is a ceramic material. However, for other applications or if the membrane is a polymer or any heat-sensitive material, heating steps may have to be avoided and other methods such as evaporation or plasma enhanced chemical vapor deposition (PECVD) are required.

The synthesis of porous thin films can also be achieved by using template procedures. An easily removable material (usually organic) serves to incorporate the inorganic component with a defined morphology, being then removed by combustion or similar methods.[10,16,17] After removing the template, voids are left in the inorganic or ceramic part of the porous film, thus defining a microstructural arrangement that replicates the distribution of the template. Usually, the removal of the template requires a heating stage with the aforementioned inconveniences.

The method described in this article for the deposition of porous thin films resembles the template approach described above. Thus, an organic material that acts as a sacrificial layer is used in the procedure. This organic material is removed simultaneously to the deposition of the silicon dioxide by PECVD.

Preparation of porous SiO_2 coatings in photovoltaic cells by PECVD has recently been reported.[2] The synthesis was carried out in a microwave reactor with SiH_4 as a precursor of Si and N_2O as plasma gas. The control of porosity of these thin films was achieved by adjusting deposition parameters such as the geometry of the reactor, pressure during deposition, etc. However, these variables mainly act by altering the gas phase deposition and agglomeration, so that porosity results from the accumulation of oxide aggregates coming from the gas phase. However, in such a case the obtained layers usually have poor mechanical properties. Also, remote PECVD has been a widely utilized procedure for deposition of SiO_2,[18–20] although the main purpose of these works was not the preparation of thin films with controlled porosity.

In the present article, we propose a PECVD procedure for the room temperature synthesis of porous oxide thin films.[21] The method provides an effective control of film porosity within a large range of values. The procedure consists of the deposition of an organic material that is subsequently removed during the formation of the SiO_2 film. The porosity correlates with the thickness of the organic and oxide layers. The final oxide thin films have good adhesion and mechanical stability, even when the films' porosity is very high. A critical point of this procedure is the requirement that both deposition of the inorganic layer and removal of the organic polymer occur simultaneously. This is accomplished by depositing an organic layer with a high oxygen concentration. Recently, we have reported on the PECVD deposition of such an organic thin film by using oxygen and toluene as precursors.[22]

This article describes the experimental procedure and presents some results of the characterization of porous SiO_2 thin films with different porosities and light scattering properties. These films have been obtained by changing the relative thickness of the organic and inorganic layers. A set of applications of these thin films are also reported to demonstrate the ample variety of porous structures that can be tailored by this method of synthesis. Thus, transparent SiO_2 thin films are examined as antireflective coatings, while SiO_2 thin films with very high porosities and low densities are used for the modification of diffusion properties of commercial membranes. Finally, a phenomenological model is proposed that accounts for the development of porosity during growth based on the characterization of the porous SiO_2 films and their growth rate.

II. EXPERIMENT

A. Preparation of porous SiO_2 thin films

The PECVD procedure to control the porosity of the SiO_2 thin films consists of the deposition of intermediate polymeric oxygenated layers (C_xO_y:H), and subsequently, SiO_2 thin films. The polymeric layer is easily removed by plasma oxidation under the experimental conditions utilized for the deposition of SiO_2. Several deposition cycles are carried out sequentially to control the porosity of the films. In each cycle, an organic film and a SiO_2 thin film are deposited.

Deposition of oxygen-rich organic layers and porous SiO_2 thin films are carried out sequentially in the same reactor. It consists of a remote microwave plasma source (SLAN) supplied with magnets to achieve electron cyclotron resonance (ECR) working conditions. This source is separated from the deposition chamber by a metallic grid preventing the microwave irradiation of the substrates. The distance from the substrates to the grid is ~10 cm. Basically, the SLAN system consists of an annular waveguide (ring resonator) with axial slot antennas positioned azimuthally at regular intervals of the waveguide's inner side. The ring resonator surrounds the plasma chamber that consists of a quartz bell jar with a diameter of 16 cm and a height of 20 cm. An ion concentration of 10^{11} cm^{-3} is achieved at the SLAN center. The concentration decays downstream and the average electron density and energy shows the same behavior. An estimation of ion concentration and average electron energy close to the substrate position gives values of 10^9 cm^{-3} and 1 eV, respectively. Typical ion energies range from 5 to 10 eV. Under these working conditions, a sheath potential results in the substrate where it is expected that a very low energy ion bombardment induces minimum damage. A more detailed description of the source and experimental setup has been published previously.[22–25] The source is fitted to a deposition chamber, where a base pressure lower than 10^{-6} Torr can be obtained with a turbomolecular pump. The toluene and $Si(CH_3)_3Cl$ flows were dosed over the sample holder with a shower-type annular dispenser placed 6 cm from the substrate to ensure its homogeneous spatial distribution. Oxygen was dosed directly into the plasma source. Oxygen, toluene, and $Si(CH_3)_3Cl$ flows were controlled with mass flow controllers. The organic and the SiO_2 layers were prepared under completely different working conditions of the source, although in both cases a plasma of oxygen was used to induce the deposition. SiO_2 thin films were deposited at 2

$\times 10^{-2}$ Torr using 5 sccm of the organosilicon precursor, 20 sccm of oxygen, and 200 W of microwave power.[24]

Deposition of the organic sacrificial layer was possible only when the working parameters were adjusted around the following values: microwave power 600 W, oxygen/toluene flow ratio 4:1, and total pressure $\sim$1 Torr. To get these conditions, a very precise adjustment was required of the mass flow controllers and the pumping capacity of the system, this latter with a throttle valve placed prior to a primary pump. At lower pressures, the organic layer was always burned out by the oxygen plasma and no deposition of the organic polymer was detected. The material of the organic layer was a highly oxygenated polymer with a high concentration of COO-, C=O, and C–OH groups. An important characteristic of this polymeric-like thin film is that it is easily removed by the plasma of oxygen used for SiO_2 deposition. Under these conditions, an etching rate of about 200 nm/min was determined for the polymer. This value is lower than rates selected for the deposition of the silicon oxide ($\sim$16 nm/min).[24] It seems critical that this sacrificial layer has a very high O/C ratio and, consequently, that the PECVD protocol of preparation of this polymeric layer utilizes an oxygen rich plasma. More details about the synthesis, characterization and properties of these highly oxygenated polymeric thin films, including their etching properties under oxidizing plasma treatments, have been published recently.[22]

B. Chemical and microstructural characterization

Chemical and microstructural characterization of the thin films was studied using several techniques. Chemical analysis was carried out by Rutherford backscattering spectroscopy (RBS), electron recoil detection analysis (ERDA), and x-ray photoelectron spectroscopy (XPS). Fourier-transform infrared spectroscopy (FTIR) was also used to verify the removal of organic functional groups after deposition of the inorganic silicon dioxide. Meanwhile, assessment of microstructure was done by observation of samples by scanning electron microscopy (SEM), atomic force microscopy (AFM), and the measurement of gas adsorption isotherms with a quartz crystal microbalance (QCM).

RBS and ERDA measurements of porous SiO_2 thin films deposited on polished Si(100) wafers were performed at the Ion Accelerator ARAMIS (Orsay, France) by using 1.5 and 3.0 MeV α^{++} particles, respectively. The RBS spectra were recorded in channeling conditions. The quantification of the measured ion spectra was performed by means of the RUMP code.

XPS spectra were acquired in a VG-ESCALAB 210 spectrometer working in the constant pass energy mode with a value of 20 eV. Unmonochromatized Mg Kα radiation ($h\nu = 1253.6$ eV) was used as excitation source.

FTIR spectra in the 400–4000 cm^{-1} energy range were collected in transmission mode at normal incidence in a Nicolet 510 spectrometer for samples deposited on intrinsic Si wafers.

Images of the surface of the porous SiO_2 thin films deposited on Si(100) wafers were taken with a JEOL-JSM5400 SEM microscope after metallization of the surface of the samples. Cross-section SEM images were also obtained for SiO_2 thin films deposited on either aluminum foil or Si(100) wafers properly cut for examination. The thicknesses of the films were obtained from either these cross-sectional SEM images and also by using a DekTak profilometer. AFM surface images were also obtained in air by using a Topometrix Explorer microscope working in the noncontact mode. Both topographic (constant force) and direct signal (constant height) images were acquired. The cantilever, with a spring constant of 42.6 $N\,m^{-1}$, was oscillated at 130 kHz. Amplitude reduction was monitored while the surface was scanned at a typical rate of one line per second. The scanner was calibrated in X, Y, and Z directions with gratings provided with the equipment.

Adsorption isotherms were measured by means of a QCM in a temperature controlled vacuum chamber. In this case, porous SiO_2 thin films were deposited on the quartz oscillators used in the QCM. Thus, toluene adsorption isotherms were measured at 292 ± 0.8 K. This procedure has been previously applied for the characterization of thin films and provides a qualitative assessment of their porous structure.[26,27]

C. Optical and gas diffusion properties

Porous SiO_2 thin films can find applications as optical coatings and gas diffusion membranes.

Ultraviolet-visible (UV-vis) transmission spectra at normal incidence of samples deposited on glass plates were obtained with a Shimadzu UV-2101PC spectrometer.

Measurements of gas diffusion through porous SiO_2 thin films acting as membranes were carried out in a homemade apparatus consisting of two chambers (chambers 1 and 2) separated by the membrane. The experimental procedure to get the permeability of a membrane to a gas A (Π_A) was the following. Chamber 2 was set initially under vacuum and chamber 1 under a certain pressure of a gas (P_1). Then, the variation of the pressure with time in chamber 2 ($\Delta P_2/\Delta t$) was monitored. In these conditions, Π_A can be determined using the equation[12,28]

$$\Pi_A = \frac{d}{A(P_1 - P_2)} \frac{V_2}{RT} \frac{\Delta P_2}{\Delta t},$$

where d is the thickness of the membrane, V_2 is the volume of chamber 2, A the membrane area, T is the temperature, and R the ideal gas constant. The ideal separation factor of a membrane for two gases A and B, α_B^A, can be determined as $\alpha_B^A = \Pi_A/\Pi_B$. To carry out this analysis, the porous silicon dioxide thin films were deposited on commercial alumina porous substrates Anodisc 47 from Anopore with nominal pore sizes of 100 and 20 nm (in the following Anodisc-100 and Anodisc-20, respectively).

III. RESULTS AND DISCUSSION

A. Composition of the porous silicon oxide thin films

The method of preparation of porous SiO_2 thin films consists of depositing the silicon oxide by PECVD using ECR

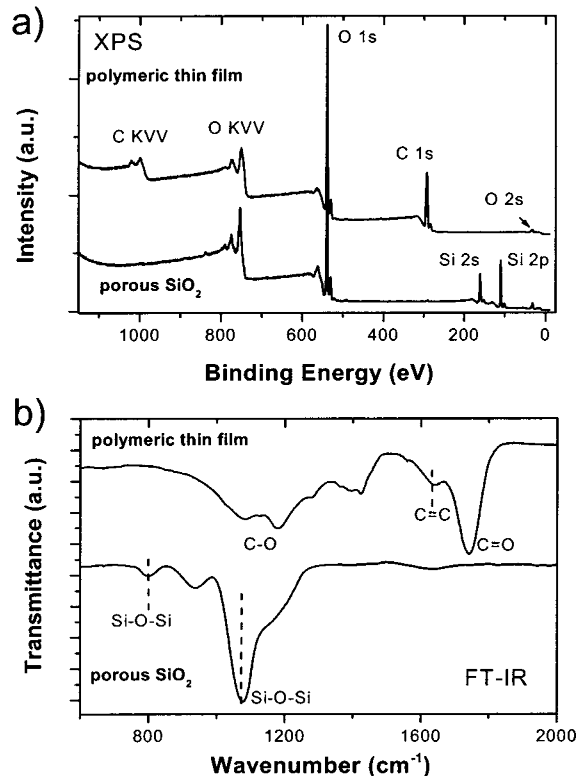

FIG. 1. (a) XPS spectra of a sacrificial organic layer of ~45 nm thick and the film resulting from the deposition of a ~220 nm SiO_2 thin film on top it. (b) FTIR spectra for the same samples.

conditions that are very effective for the complete removal of a previously deposited organic sacrificial layer. It is critical that during this process, total removal of the organic layer is accomplished and that, therefore, the final SiO_2 thin film is free from any organic contaminant. Survey XPS spectra of the sacrificial organic layer and after deposition of a SiO_2 layer on this sacrificial layer are shown in Fig. 1(a). Note that the sacrificial layer shows only peaks due to C and O atoms that evidences the presence of a highly oxygenated organic layer. After deposition of the SiO_2 film, the C1*s* peak disappears from the spectrum, indicating that no carbon contamination remains in the sample. Moreover, only peaks attributed to silicon (in particular Si^{4+} species) and oxygen atoms can be seen in this spectrum.

Since XPS is a surface sensitive probe, we have also used channeling RBS to prove the absence of carbon in the SiO_2 layers. Thus, we found that the bulk compositions of the films are stoichiometric silicon dioxide and that their carbon content is below the detection limit of this technique.

Figure 1(b) shows the FTIR spectra corresponding to the sacrificial layer (top) and a SiO_2 deposit on this sacrificial layer (bottom). In the FTIR spectrum of the sacrificial layer there are signals due to C and O groups[22,29] (i.e., C—O, C═O, C═C, etc.) typical of a highly oxygenated organic polymeric layer. After silicon oxide deposition, the signals of carbon-oxygen groups completely vanish, indicating that no carbon remains in the sample after this treatment. Note also that, the FTIR spectrum after removal of the organic groups depicts the typical bands of SiO_2.[24,30,31]

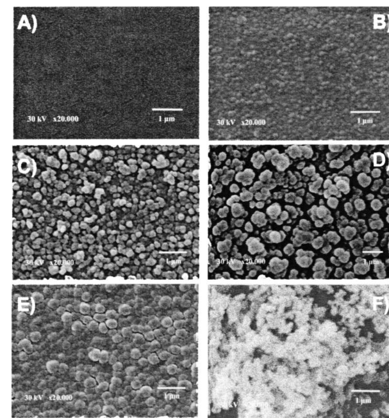

FIG. 2. SEM micrographs of SiO_2 thin films with increasing porosities. The preparation protocols of samples A–F are reported in Table I.

B. Microstructure of the SiO_2 thin films

Control of the porosity of the SiO_2 thin films is achieved by adjusting the thicknesses of the polymeric C_xO_y:H and SiO_2 layers. As an example of the possibilities of the method, Figs. 2(a)–2(d) shows a series of SEM micrographs of SiO_2 thin films with a similar total thickness of ~600 nm but increasing porosity. These samples have been prepared by different preparation protocols consisting of two cycles of deposition. In each cycle, an organic thin film (i.e., the polymeric C_xO_y:H described below) and a SiO_2 thin film are deposited. The preparation protocols of these samples are shown in Table I. Deposition is carried out in two steps and the thickness of the organic and inorganic materials has been adjusted to achieve the desired porosities. It is apparent in this set of micrographs that, for a constant thickness of the final SiO_2, the porosity increases as the thickness of the organic phase increases.

However, for the same thickness of the sacrificial organic layer, the final microstructure of the films also depends on the final thickness of the oxide film. An example of the effect of the thickness of the intermediate oxide films in the final microstructure of the porous films is evidenced by the comparison of Figs. 2(d) and 2(e). The corresponding films are obtained by two cycles with similar polymeric films, but different thickness of the final oxide films (cf. Table I). It is possible to see that as the thickness of the oxide layers increases, the percolation degree of the individual aggregates (i.e., the degrade of interconnection among them) of the layer increases and the final structure at the surface becomes more compact.

It can be also seen in this figure that the percolation degree of the SiO_2 aggregates is relatively high, and the pore size small, when the oxide is deposited on top of an organic layer of ~25 nm [i.e., Fig. 5(b)]. For an organic layer thinner than approximately 25 nm, the final SiO_2 thin films, although still having much porosity, are transparent and do not present any observable light scattering. However, SiO_2 films pre-

TABLE I. Preparation protocols of selected porous SiO_2 samples.

Sample	Step 1	Step 2	Substrate	Density (g/cm^3)	Porosity (%)
A	600 nm SiO_2	–	Si(100)	1.98	10.0
B	25 nm C_xO_y:H+ 150 nm SiO_2	25 nm C_xO_y:H+ 450 nm SiO_2	Si(100)	1.66	24.6
C	40 nm C_xO_y:H+ 150 nm SiO_2	40 nm C_xO_y:H+ 450 nm SiO_2	Si(100)	1.25	43.2
D	60 nm C_xO_y:H+ 150 nm SiO_2	60 nm C_xO_y:H +450 nm SiO_2	Si(100)	1.10	55.4
E	60 nm C_xO_y:H+ 475 nm SiO_2	60 nm C_xO_y:H+ 475 nm SiO_2	Si(100)	1.56	29.4
F	250 nm C_xO_y:H+ 150 nm SiO_2	250 nm C_xO_y:H+ 375 nm SiO_2	Si(100)	0.78	64.5
G	40 nm C_xO_y:H+ 275 nm SiO_2	40 nm C_xO_y:H+ 275 nm SiO_2	Al sheet	–	–
H	7 cycles (50 nm C_xO_y:H+275 nm SiO_2)		Al sheet	–	–

pared after deposition of thicker organic films had a milky appearance due to light dispersion in the individual aggregates or columns of SiO_2.

The micrographs in Fig. 2 also show that by controlling the thickness of the oxide and polymeric layers, it is possible to achieve precise control of the final pore size and concentration of the films. With our procedure, successive deposition of different oxide layers with specific and tailored porosity would permit the fabrication of thin films with variable in-depth porosity and optical properties. This type of thin film with gradient porosity is of interest for certain type of optical filters, the so-called rugate filters.[32,33]

The microstructure of the SiO_2 samples was of the columnar type in all cases, except when deposited on top of a very thick organic film (i.e., 250 nm). In this case, Fig. 2(f) shows that the film has a granular microstructure. This sample is the result of the aggregation of small powdered particles and, therefore, this film's mechanical stability was very poor. To illustrate the columnar growth of the porous thin films, Fig. 3 shows two cross-sectional views of SiO_2 samples deposited on an aluminum foil. Both views depict a well-defined columnar microstructure. Sample G in this figure corresponds to a film deposited by two cycles C_xO_y:H polymer/SiO_2, while sample H corresponds to a thick film obtained after seven cycles of deposition of organic and inorganic layers (cf. Table I). The micrograph of this latter sample clearly shows that a common columnar microstructure develops independently of the final thickness of the films (i.e., ~500 and ~2850 nm for the films shown in Figs. 3(g) and 3(h), respectively) and of the number of cycles used for deposition of the film. No boundary interfaces between the intermediate individual SiO_2 layers can be detected in sample G. This proves that the final porous thin films are homogeneous in thickness, even for several deposition-removal steps of the sacrificial organic layers.

A similar microstructure to that reported in Fig. 3, with vertical pores and columns, was found for all the samples, although the pore size and type of columns depend on the actual preparation conditions used in each case. Such a columnar microstructure does not develop in the SiO_2 films deposited at 2×10^{-2} Torr without deposition of the intermediate polymeric films (i.e., sample A in Table I). The development of columns in the porous thin films is justified by a phenomenological model described below.

AFM images were taken to study the surface morphology and growing mechanisms of the porous SiO_2 thin films. Figure 4(a) shows the surface of a dense SiO_2 thin film (i.e., prepared without mediation of the intermediate organic layer) of ~110 nm thickness and Fig. 4(b) that of an porous oxide film of a similar thickness grown onto a previously deposited organic layer of ~25 nm. At first glance, the

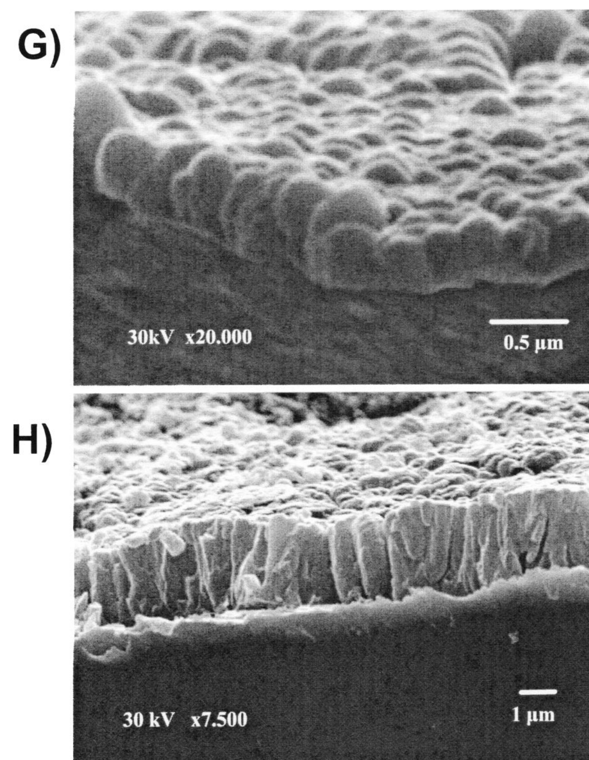

FIG. 3. Cross-sectional SEM micrograph corresponding to samples G and H in Table I.

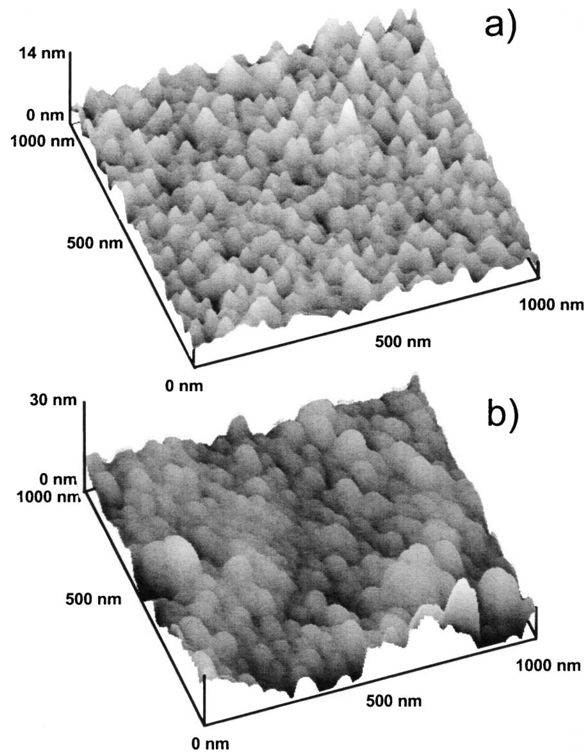

FIG. 4. AFM images of dense (a) and porous (b) SiO_2 thin films prepared by PECVD. The films have a thickness of ~100 nm. The porous layer has been prepared according to the protocol 20 nm C_xO_y:H+ 100 nm SiO_2.

latter depicts a more corrugated aspect than the former. The statistical analysis of the particle size distributions, depicted in Fig. 5 in the form of bearing plots, shows that the mean size of the aggregates in the porous sample is higher by 11.5 nm than that in the compact thin film, although the size dispersion profiles are similar in both cases. A rather homogeneous size distribution points to a growth mechanism controlled by the aggregation of material to a given number of initially formed nuclei and not to a complex process involving both growth of particles and formation of new nuclei.

The density ρ of the films was determined from the Si, O, and H atomic surface concentration (by means of channeling-RBS and ERDA measurements) and the film

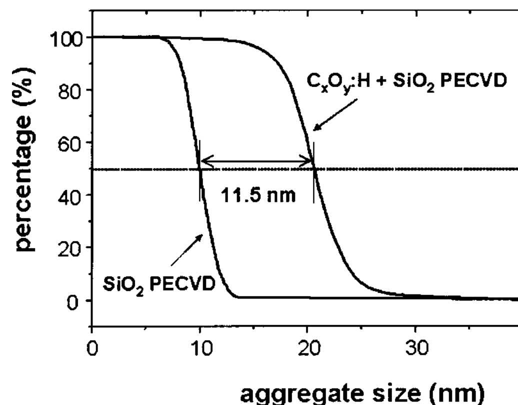

FIG. 5. Bearing plots of samples whose AFM images are reported in Fig. 4.

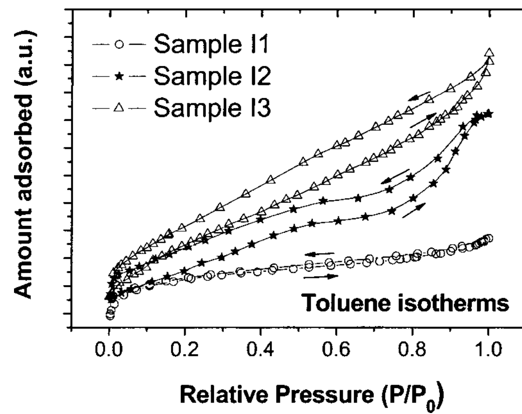

FIG. 6. Selected adsorption/desorption isotherms of toluene vapor on porous thin films I1, I2, and I3 (see text).

thickness obtained by cross-sectional SEM images and/or profilometry. The porosity Γ of each film was calculated using the relationship $\Gamma = 100\times(1-\rho/\rho_s)$, where ρ_s corresponds to the density of compact bulk silica[34] ($\rho_s = 2.20\ \mathrm{cm^3/g}$). Our results show that it is possible to control the density of the SiO_2 films in the range 1.98–0.65 g/cm^3, i.e., a set of values which corresponds to porosities from 10% to 65%. Table I lists the density and porosity of the films whose SEM micrographs have been shown in Fig. 2. The reported values clearly prove that for a fixed thickness of the intermediate oxide film used in the cycles, the thicker the organic sacrificial layer, the larger the porosity, and the smaller the density of the porous silicon oxide thin films.

The analysis of the adsorption–desorption isotherms of a gas or vapor in a material provides information about its porous microstructure.[35] In the present work, we have used a QCM to measure gas adsorption isotherms in our thin films according to the procedure described in the experimental section. A similar procedure has been used for the analysis of porosity of silica thin films using nonpolar adsorbates.[26,27] Figure 6 shows three selected adsorption/desorption isotherms of toluene carried out on three thin films with well differentiated adsorption properties. The isotherms correspond to samples I1 (3 cycles of 8 nm C_xO_y:H+300 nm SiO_2), I2 (4 cycles of 30 nm C_xO_y:H+150 nm SiO_2), and I3 (4 cycles of 70 nm C_xO_y:H+100 nm SiO_2). The shapes of the isotherms of samples I1, I2, and I3 in Fig. 6 are close to types I, IV and II of The International Union of Pure and Applied Chemistry (IUPAC) classification,[35] respectively. According to this classification, the pores are characterized by their average width w, i.e., the diameter of a cylindrical pore, or the distance between the sides of a slit-shaped pore. Type II and IV isotherms are indicative of macroporosity ($w \geqslant 50$ nm) and mesoporosity ($2 \leqslant w \leqslant 50$ nm), respectively. Both isotherms have hysteresis loops that approach to the type H_3 of the IUPAC classification for isotherms with hysteresis loops. This type of hysteresis is characteristic of the adsorption in slit-shaped pores.[35] It is therefore likely that the pores between the columns that define the microstructure of the films

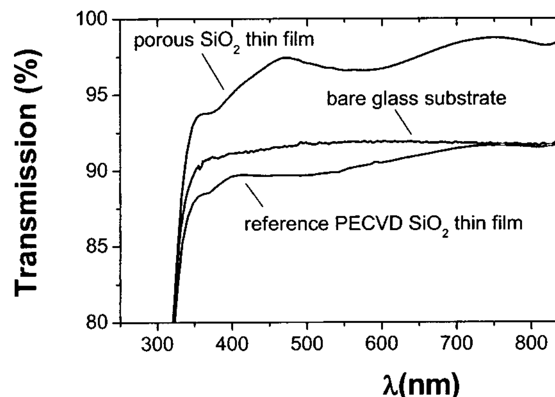

FIG. 7. UV-Vis spectra of a bare glass substrate and this substrate covered by a compact and a porous SiO_2 thin films.

I2 and I3 are responsible for the shape of the hysteresis loops found for the isotherms of these two samples. By contrast, sample I1 presents a smaller porosity with practically no hysteresis loop between the adsorption and desorption branches of the isotherm. This isotherm is close to type I of the IUPAC classification and the pore size falls within the range of micropores ($w<2$ nm). Therefore, from this analysis of isotherms, it is concluded that the present PECVD method provides an effective control of the porosity of thin films in the range of macro-, meso-, or micro-pores.

C. Potential applications

1. Porous SiO_2 thin films as antireflective coatings

The incorporation of porous SiO_2 thin films as antireflective coatings has been claimed as a possible way to increase the light transmission through glass or polymer covers used in photovoltaic modules and other applications in optics.[2,3] An increase in the light transmission coefficient is expected when a layer with a low refractive index is deposited on these substrates. With our method, transparent porous SiO_2 thin films with negligible light dispersion are prepared when using sacrificial organic layers thinner than ~25 nm.

To demonstrate the antireflective character of the SiO_2 thin films prepared with our method, we have measured the UV-vis spectra of a glass plate covered with such a thin film. Figure 7 shows three UV-vis absorption spectra corresponding to a bare glass plate, to one-side of this plate covered by a dense 500 nm SiO_2 thin film prepared directly by PECVD, and to a porous SiO_2 thin film deposited by two cycles C_xO_y:H/SiO_2 (i.e., 5 nm C_xO_y:H, 150 nm SiO_2 + 5 nm C_xO_y:H, 375 nm SiO_2). In this latter case, an enhancement of about 7%–8% transmission occurs for the whole range of visible wavelengths. Such an effect is not observed when a compact SiO_2 layer is deposited without intermediate polymeric films [cf., Fig. 2(a)], for which the transmission is lower than that of the bare glass plate.

Although similar results have been reported recently for SiO_2 thin films prepared by PECVD in a rf setup,[2] the advantage of the method reported here relies on the fact that the porosity is controlled in a reproducible way within a very large set of values.

2. Porous SiO_2 thin films as gas-diffusion membranes

Another possible application of porous thin films is as membranes for separation of fluids. Here we present a preliminary characterization of the gas-diffusion behavior of some SiO_2 thin films. The purpose is to show that by adjusting the porosity of the films, it is possible to prepare membranes with different gas-diffusion rates.

Table II summarizes the results of gas-diffusion experiments with selected samples deposited on commercial alumina Anodisc 47 porous substrates. The table also reports the values corresponding to the bare alumina porous substrates without SiO_2 covering layer. Sample M1 in the table corresponds to a SiO_2 sample of ~800 nm thickness prepared by PECVD at 2×10^{-2} Torr without any intermediate sacrificial layer [i.e., similar to the sample whose SEM micrograph is shown in Fig. 2(a)]. The low gas permeability found for this sample indicates that the film is compact and grows without cracks and voids onto the porous alumina substrates. This compact SiO_2 film acts as a barrier against diffusion of gases.

Similar experiments were carried out with samples of controlled porosity (cf. Table II). Thin films M2 and M3, with a thickness of ~500 nm, were deposited on the Anodisc-100 substrates. The preparation protocols of these two samples differ in the thickness of the organic layer, with 100 nm for sample M2 and 65 nm for sample M3. Both samples have been prepared with two cycles of ~200 and ~300 nm of SiO_2, respectively. As expected, the permeability of sample M2 is about 10%–20% higher than that of

TABLE II. Permeability Π (mol m^{-1} s^{-1} Pa^{-1}) to several gases of selected SiO_2 membranes deposited on Anodisc 47 substrates. The ideal separation factor of the membranes for CH_4 and CO_2, $\alpha^{CH_4}_{CO_2}$ is also included.

Film/substrate	H_2	CH_4	C_3H_6	Kr	$\alpha^{CH_4}_{CO_2}$
M1/Anodisc-20	1.4 10^{-13}	3.1 10^{-14}	2.2 10^{-14}	–	–
M2/Anodisc-100	7.6 10^{-10}	3.3 10^{-10}	2.4 10^{-10}	1.5 10^{-10}	1.60
M3/Anodisc-100	6.3 10^{-10}	2.6 10^{-10}	1.8 10^{-10}	1.4 10^{-10}	1.62
M4/Anodisc-20	4.4 10^{-10}	1.8 10^{-10}	1.3 10^{-10}	7.7 10^{-11}	1.58
M5/Anodisc-20	8.6 10^{-13}	–	1.6 10^{-13}	1.0 10^{-13}	–
Anodisc-20	9.0 10^{-10}	–	2.2 10^{-10}	1.7 10^{-10}	–
Anodisc-100	–	–	–	>3 10^{-9}	–

sample M3, although the permeability of both samples is much smaller than that of the Anodisc-100 substrate (cf. Table II). The permeabilities of samples M2 and M3 are even lower than those found for the Anodisc-20 substrate. These results evidence the possibility of adjusting the transport properties of commercial bulk membranes by depositing thin porous layers on their surface.

Samples M4 and M5 in Table II have a thickness of ~750 nm and were deposited on Anodisc-20 substrates. They were prepared using two intermediate organic layers 60 and 4.5 nm thick, respectively. In the first case, the decrease in gas permeability was higher than for samples M2 and M3, reaching a percentage of 40%–55%. In the case of sample M5, it is possible to observe in the table a dramatic decrease in the gas permeability of several orders of magnitude. Many procedures have been reported in the literature to restrict the flow of gases through bulk porous membranes. For example, methods have been reported that consist of depositing different oxide thin films by thermal chemical vapor deposition (CVD) or the impregnation with colloidal SiO_2 particles.[36–40] The deposition of either compact or porous SiO_2 thin films by PECVD according to the present procedure may be an interesting alternative to these methods, particularly when no heating step during preparation is required. In this sense, it could also be expected that our method, furnishing an arrangement of pores perpendicular to the surface, could be an alternative to the anodic oxidation used commercially for the synthesis of supports with controlled permeability.[7,40]

Table II also reports the separation coefficients for CO_2 and CH_4 through the different films. The obtained values are rather similar for the four samples M2, M3, and M4, indicating that within the degree of porosity studied here, the selectivity for these two gases is practically the same. This behavior is expected when diffusion of gases occurs through membrane thin films whose porous size falls within the range of mesopores.[8,12,40]

D. Growth mechanism of porous SiO_2 thin films

Porosity in SiO_2 or other metal oxide thin films prepared by plasma CVD procedures is usually controlled by adjusting the pressure during deposition and/or by modifying geometrical parameters of the plasma reactor, such as distance between the shower dispenser and the substrate.[2] These changes modify the condensation processes of oxide particles in the gas phase. Thereby, porosity is controlled by the different size of particles and nuclei coming from the plasma. Deposition of porous SiO_2 thin films by accumulation of aggregates was also possible with our reactor setup by using $Si(CH_3)_3Cl$ as precursor and oxygen as plasma gas, with a working pressure over 0.5 Torr. Under these conditions, gas phase deposition processes were maximized and the film grew by the accumulation of powder particles. However, these films had very poor mechanical properties.

The sacrificial layer method relies on a different concept. A polymeric-organic film is plasma oxidized and removed simultaneously to the deposition of the inorganic SiO_2 layer.

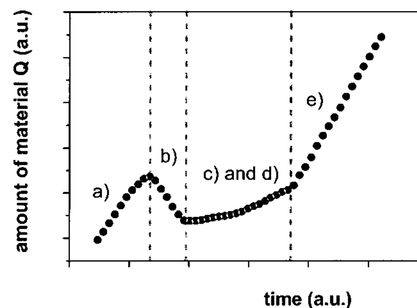

FIG. 8. Evolution of the amount of material Q deposited on a quartz oscillator and detected with a QCM during deposition of the sacrificial organic layer and posterior deposition of the SiO_2 thin film (see text).

Although a model of the SiO_2 deposition cannot be fully outlined at the present stage, we can consider several phenomena which, under our experimental conditions, are likely to control the final porosity. The first is the modification of the nucleation and initial growth steps of SiO_2 because of the presence of the organic layer. The fact that this organic film is formed by highly oxygenated carbonaceous chains seems critical to provide access pathways to the substrate surface to activated precursor molecules and other species of the plasma. A critical clue for the process is that the polymeric layer is easily removed by plasma oxidation under the ECR conditions utilized for SiO_2 deposition.[22] Under these conditions, the polymer etching rates are about ten times higher than the deposition rate of the SiO_2 layers. This means that deposition of the inorganic film mainly occurs when the polymeric layer has already been burned off. Figure 8 shows a plot of the amount of material Q deposited on the quartz oscillator during a deposition cycle of an organic layer followed by the SiO_2 material. Initially, during the initial deposition of the organic layer, Q increases (a). Then, during the initial stages of deposition of the SiO_2 (b), Q decreases, thus indicating that the removal of the organic layer is the predominant process. The zone where Q decreases is followed by the other with a smooth increase of Q (c) and (d) that ends up with a last region with a sharp increase of Q (e). The latter indicates a net deposition of the SiO_2 without interference by any other removal process. We assume that the intermediate zones (b)–(d), characterized first by a negative slope and then by a small positive slope, reflect a sequence of the experiment where etching of the organic layer and deposition of the inorganic oxide take place simultaneously. With respect to this behavior, it is important to stress the importance of using sacrificial organic layers which can be efficiently removed by plasma etching. Experiments carried out in our laboratory with other sacrificial layers which are burned out more slowly show the formation of sandwich structures where the organic layer is embedded within an oxide layer with less porosity than that of the porous thin films described in the previous sections.

Taking into account the results of Fig. 8 obtained during each cycle of deposition of the porous SiO_2 thin films, Fig. 9 shows a schematic description of a mechanism which is proposed to account for the evolution of the microstructure of

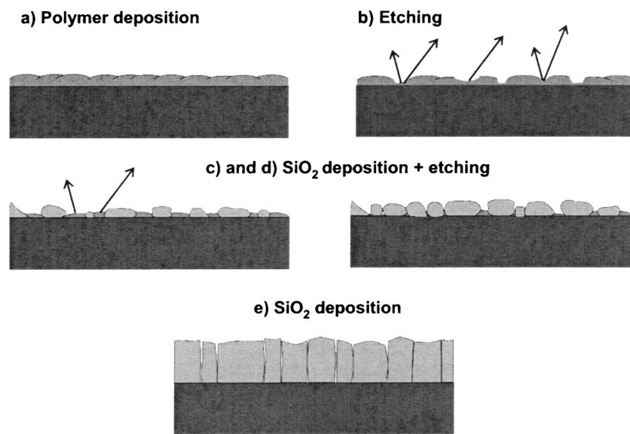

FIG. 9. Proposed scheme for the deposition process of a porous SiO_2 layer over a previously deposited sacrificial organic layer (see text).

these films. The SiO_2 deposition is initiated on a substrate fully covered by an organic layer (a). In the initial stages of SiO_2 deposition, fast removal of this sacrificial layer takes place (b). At the same time, SiO_2 starts to nucleate at certain sites of the substrate that are becoming free from the polymeric material (c) and (d). The columnar growth of the inorganic oxide (e) will be much influenced by the effectiveness of the removal of the organic material, so that the final microstructure will depend on a very delicate balance of different factors like shadowing, restriction of mobility of adatom species of silicon, release of gases (CO_2,H_2O) produced by oxidation of the organic film, etc. Depending on the relative importance of these factors and the characteristics of the initially formed nuclei (i.e., size, dispersion, etc.), growth of the silicon dioxide film occurs in different ways and leads to different microstructures.

IV. CONCLUSIONS

The presented results show that it is possible to control the microstructure of oxide thin films deposited by room temperature PECVD by using sacrificial polymeric organic layers. The method is very versatile and permits to tailor a large variety of pore microstructures as required for many applications, from optical films to gas diffusion membranes and supports. This method extends the synthesis of oxide films by PECVD to the preparation of porous films with a columnar porous structure perpendicular to the surface and enables the deposition of porous thin films on polymers and other substrate sensitive to high temperatures.

Preliminary studies have shown that other oxide materials besides SiO_2 can be deposited in the form of porous thin film following a similar procedure. This opens the possibility of preparing porous thin film structures of mixed and/or gradient compositions. This ability, together with the in-depth control of porosity which is another key feature of the method, could permit the tailoring synthesis of thin films where both composition and porosity can be simultaneously and independently controlled.

Since the preparation protocol is based on a PECVD procedure, the method is compatible with the silicon technology (e.g., as low-*k* materials).

ACKNOWLEDGMENTS

The authors thank C. Clerc from the Ion Accelerator ARAMIS (Orsay, France) for her assistance with the RBS measurements, J. Benítez from ICMSE (Sevilla, Spain) for the AFM images, and the financial support of the Spanish Ministerio de Ciencia y Tecnología (Project No. MAT2001-2820) and the EU (Project No. ENV4-CT97-0633 and the MULTIMETOX network).

[1] I. M. Thomas, Appl. Opt. **31**, 6145 (1992).
[2] H. Nagel, A. Metz, and R. Hezel, Sol. Energy Mater. Sol. Cells **65**, 71 (2001).
[3] G. Helsch, E. Rädlein, and G. H. Frishat, J. Non-Cryst. Solids **265**, 193 (2000).
[4] J. K. Hong, H. S. Yang, M. H. Jo, H. H. Park, and S. Y. Choi, Thin Solid Films **308–309**, 495 (1997).
[5] A. Jain, S. Rogojevic, S. Ponoth, N. Agarwal, I. Matthew, W. N. Gill, P. Persans, M. Tomozawa, J. L. Plawsky, and E. Simonyi, Thin Solid Films **398**, 513 (2001).
[6] J. K. Hong, H. R. Kim, and H. H. Park, Thin Solid Films **332**, 449 (1998).
[7] H. P. Hsieh, Catal. Rev. - Sci. Eng. **33**, 1 (1991).
[8] W. J. Koros and G. K. Fleming, J. Membr. Sci. **83**, 1 (1993).
[9] A. B. Shelekhin, S. Pien, and Y. H. Ma, J. Membr. Sci. **103**, 39 (1995).
[10] L. Cot, A. Ayral, J. Durand, C. Guizard, N. Hovnanian, A. Julbe, and A. Larbot, Solid State Sci. **2**, 313 (2000).
[11] A. Ohl and K. Schröder, Surf. Coat. Technol. **116–119**, 820 (1999).
[12] D. R. Lloyd, editor, *Material Science of Synthetic Membranes* (American Chemical Society, Washington, DC, 1985).
[13] P. Liu, S. H. Lee, C. Edwin Tracy, Y. Yan, and J. A. Turner, Adv. Mater. (Weinheim, Ger.) **14**, 27 (2002).
[14] P. D. Yang, D. Y. Zhao, D. I. Margolese, B. F. Chmelka, and G. D. Stucky, Nature (London) **396**, 152 (1998).
[15] P. D. Yang, D. Y. Zhao, D. I. Margolese, B. F. Chmelka, and G. D. Stucky, Chem. Mater. **11**, 2813 (1999).
[16] N. K. Raman, M. T. Anderson, and C. J. Brinker, Chem. Mater. **8**, 1682 (1996).
[17] I. Honma, H. S. Zhou, D. Kundu, and A. Endo, Adv. Mater. (Weinheim, Ger.) **20**, 1529 (2000).
[18] A. Grill, *Cold Plasma in Materials Fabrication* (Wiley-IEE Press, 1994).
[19] G. Lucovsky and D. V. Tsu, J. Vac. Sci. Technol. A **5**, 2231 (1987).
[20] D. Korzec, D. Theirich, F. Werner, K. Traub, and F. Engemann, Surf. Coat. Technol. **74–75**, 67 (1995).
[21] A. Barranco, F. Yubero, J. P. Espinós, A. R. González-Elipe, and J. Cotrino, *Procedure for the Preparation of Porous Thin Films of Inorganic Oxides* (ref. Spanish patent 200100911, 19th April 2001; PCT ES02/00192).
[22] A. Barranco, J. Cotrino, F. Yubero, and A. R. González-Elipe, J. Vac. Sci. Technol. A **21**, 1655 (2003).
[23] F. Werner, D. Korzec, and J. Engemann, Plasma Sources Sci. Technol. **3**, 473 (1994).
[24] A. Barranco, J. Cotrino, F. Yubero, J. P. Espinós, J. Benítez, C. Clerc, and A. R. González-Elipe, Thin Solid Films **401**, 150 (2001).
[25] J. Cotrino, A. Palmero, V. Rico, A. Barranco, J. P. Espinós, and A. R. González-Elipe, J. Vac. Sci. Technol. B **19**, 410 (2001).
[26] F. N. Dultsev, L. A. Nenasehva, and L. L. Vasilyeva, Thin Solid Films **315**, 72 (1998).
[27] M. R. Baklanov, L. L. Vasylyeva, T. A. Gavrilova, F. N. Dultsev, K. P. Mogilnikov, and A. Nenasheva, Thin Solid Films **171**, 43 (1989).
[28] S. Roualdes, A. Van der Lee, R. Berjoan, J. Sanchez, and J. Durand, AIChE J. **45**, 1566 (1999).
[29] S. F. Durrant, S. G. Castro, J. I. Cisneros, N. C. da Cruz, and M. A. Bica de Moraes, J. Vac. Sci. Technol. A **14**, 118 (1996).
[30] P. Lange, J. Appl. Phys. **66**, 201 (1989).
[31] R. M. Almeida and C. G. Pantano, J. Appl. Phys. **68**, 4225 (1990).

[32]L. Martinu and D. Poltras, J. Vac. Sci. Technol. A **18**, 2619 (2000).
[33]W. H. Southwell, J. Opt. Soc. Am. A **5**, 1558 (1988).
[34]W. A. Weyl and E. C. Marbone, *The Constitution of Glasses* (Wiley-Interscience, New York, 1964).
[35]S. J. Gregg and K. S. W. Sing, Adsorption, *Surface Area and Porosity*, 2nd ed. (Academic, New York, 1997), and references therein.
[36]M. Tsapatsis and G. R. Gavalas, AIChE J. **38**, 847 (1992).
[37]M. Tsapatsis and G. R. Gavalas, J. Membr. Sci. **87**, 281 (1994).
[38]M. Moaddeb and W. J. Koros, J. Membr. Sci. **125**, 143 (1997).
[39]M. Moaddeb and W. J. Koros, J. Membr. Sci. **136**, 273 (1997).
[40]E. J. Jakobs, Ph. D. thesis, The University of Texas at Austin, University Microfilms International Dissertation Services, Ann Harbor, 1996.